

Remote Sensing of Phytoplankton Blooms in the Continental Shelf and Shelf-Break of Argentina: Spatio-Temporal Changes and Phenology

Verónica Carolina Andreo, *Member, IEEE*, Ana I. Dogliotti, and Carolina Beatriz Tauro

Abstract—We studied the spatio-temporal variations of satellite chlorophyll-a (chl-a) and phytoplankton blooms in the continental shelf and shelf-break of the Argentinean patagonic region by means of an 11-years time series of level 3 (L3) MODIS/Aqua chlorophyll products. We aggregated data according to different granularities and estimated climatologies and anomalies. We also studied the phenology of phytoplankton blooms determining bloom starting date and date of maximum concentration. Finally, we estimated and described statistical indexes such as bloom occurrence frequency. The results obtained provide an overview of the evolution and the spatio-temporal variability of chl-a that, in general, and despite its limitations, was complementary and consistent with previous studies based on both satellite and *in situ* data. This study intended to set the baseline to study algal blooms and their variability in the Argentinian sea, which is valuable information to be included in predictive models related to the occurrence of harmful algal blooms, dynamics of marine system and the effects of global changes over climatic and biogeochemical cycles. In addition, this study also contributes with more up-to-date science data for the future Argentinian and Brazilian SABIA-Mar ocean color mission, which will provide high resolution data (200 m) over the Argentinian coastal zones and continental shelf. Besides the results *per se*, the relevance of this study is also related to the use of an novel free and open source tool.

Index Terms—Geographic information systems, marine vegetation, remote sensing, sea, time series.

I. INTRODUCTION

THE planktonic microscopic and photosynthesizing organisms inhabiting oceans, globally called phytoplankton, constitute the basis of all oceanic food webs and play a fundamental role in carbon cycling and biogeochemical cycles [1], and thus in global climate. Changes in phytoplankton biomass have significant impacts on all the biological, physical, and geochemical processes occurring in the aquatic system. Therefore, there has been a rising interest in studying, monitoring, and

Manuscript received March 8, 2016; revised May 21, 2016; accepted June 17, 2016. Date of publication July 19, 2016; date of current version November 30, 2016. The work of V. C. Andreo was supported by Comisión Nacional de Actividades Espaciales. (*Corresponding Author: Verónica Carolina Andreo.*)

V. C. Andreo and C. B. Tauro are with Comisión Nacional de Actividades Espaciales, Falda del Carmen 5187, Argentina and also with the Facultad de Matemática, Astronomía y Física, Universidad Nacional de Córdoba, Ciudad Universitaria, Córdoba 5000, Argentina (e-mail: veroandreo@gmail.com; carolina.tauro@conae.gov.ar).

A. I. Dogliotti is with Instituto de Astronomía y Física del Espacio (CONICET-UBA), Ciudad Universitaria, Buenos Aires 1428, Argentina (e-mail: adogliotti@iafe.uba.ar).

Color versions of one or more of the figures in this paper are available online at <http://ieeexplore.ieee.org>.

Digital Object Identifier 10.1109/JSTARS.2016.2585142

understanding these spatio-temporal variations and their phenology at the regional and global scales [2].

The Argentinian continental shelf is one of the widest and flattest continental shelves in the world ocean; it widens southward from 170 km at 38 S to about 800 km at 50 S. It is a highly dynamic region characterized by the confluence of two western boundary currents (Brazil and Malvinas currents) and the presence of several oceanographic fronts; the shelf-break front between shelf sub-antarctic waters and Malvinas Current waters and several tidal fronts which develop in spring and summer that define the border between vertically mixed and stratified shelf waters. These frontal areas have been associated with enhanced chlorophyll-a (chl-a) concentration [3], [4] and with intense CO₂ uptake from spring through autumn [5], suggesting that photosynthesis is the responsible mechanism. Because of this, the Argentinian continental shelf has been described as one of the richest areas of the world oceans both in terms of phytoplankton biomass but also for the great abundance of economically important fish and mollusk species, and sea birds and marine mammals [6].

Since algae have photosynthetic pigments, such as chl-a, which absorb and reflect sun light mainly in the visible part of the electromagnetic spectrum, phytoplankton is capable of changing the optical properties of surrounding water, that is the *ocean color*. This principle allows estimating chl-a concentration (proxy for phytoplankton biomass) through measurements of the reflected radiation from the upper ocean layer by means of remote sensing and further calibration with *in situ* data. In this sense, remote sensing of ocean color is an ideal tool to assess primary production on a regional and global scale, since it offers good spatial and temporal coverage providing almost daily estimations of the phytoplankton biomass.

Global studies using ocean-color satellite images have revealed that the Argentinian continental shelf is the region with the highest increase in chlorophyll between 1998 and 2003 [7]. The use of ocean-color satellite images in this region has increased over the past decades. The pioneering study by Brown and Podestá [8] suggesting the presence of coccolithophorids at the shelf-break was followed by that of Garcia *et al.* [9] and Signorini *et al.* [10]. There were also some studies comparing *in situ* and satellite chl-a estimates [11], [12], and others, based solely on satellite information (SeaWiFS), that have analyzed the annual patterns of chlorophyll distribution [3], [4]. However, to the best of our knowledge, level 3 (L3) MODIS products have not yet been used to address the spatial and temporal chl-a variations over the Argentinian continental shelf.

Moreover, the previous studies have covered shorter periods that reached no farther than 2004. Besides, there are no regional studies regarding anomalies in chl-a concentration nor studies about phenology of phytoplankton blooms.

The purpose of this paper is to describe the monthly and interannual variability of chl-a in the Patagonian Continental Shelf (PCS), its anomalies and the phenology of phytoplankton blooms from 2003 to 2013, by means of satellite derived ocean color data from MODIS/Aqua sensor. A secondary, but not less important, objective was to provide more up-to-date baseline information regarding the distribution of chl-a concentration over the Argentinian sea for the future SABIA-Mar ocean color mission (<http://www.conae.gov.ar/index.php/english/satellite-missions/sac-e/introduction>), which is being jointly developed by the Argentinian and Brazilian space agencies. This ocean color mission is conceived to provide information and products of coastal areas and coastal hazards, fisheries and, ocean ecosystems. In this sense, a regional characterization is valuable information for the continuity of satellite time series data.

II. MATERIALS AND METHODS

A. Data

The eight-day composite chl-a and remote sensing reflectance at 667 nm (R_{rs667}) retrieved by MODIS/Aqua were acquired from the NASA ocean color website (<http://oceancolor.gsfc.nasa.gov>). For both parameters, we used standard mapped image L3 products. The spatial resolution of both datasets is ≈ 4.6 km with global coverage and spanning the period from January 2003 to December 2013 (11 years, a total of 506 images per variable, chl-a and R_{rs667}). The NASA standard algorithms were used to derive the R_{rs667} (in sr^{-1}) and chl-a (in mg/m^3) using the OC3Mv6 algorithm. We used the eight-day composite chl-a datasets to characterize phytoplankton changes and obtain the statistics on phytoplankton blooms; and satellite-derived R_{rs667} to have a proxy of water turbidity, with larger R_{rs667} corresponding to higher water turbidity. With this latter product, we masked probable false blooming in coastal waters [13]. We chose L3 eight-day compositions of 4.6 km of spatial resolution because they are suitable to perform long term statistical characterization for wide regions, since they smooth the very high spatial and temporal variability of chl-a [14]. In turn, higher resolution products are helpful to get detailed information in the coastal zone, but they require further study and understanding given the complexity of these type of waters for which standard algorithms do not usually work. Thus, this L3 product is good enough as a first indicator of chl-a concentration variations in the large scale.

Our study region covered the PCS between 38 and 55 S and, 55 and 70 W (see Fig. 1).

B. Processing and Analyses

1) *Availability of Valid Data:* We analyzed the availability of valid data in terms of percentage of valid data for the whole period considered and climatologically for every month of the year. We also characterized the interannual variability in the

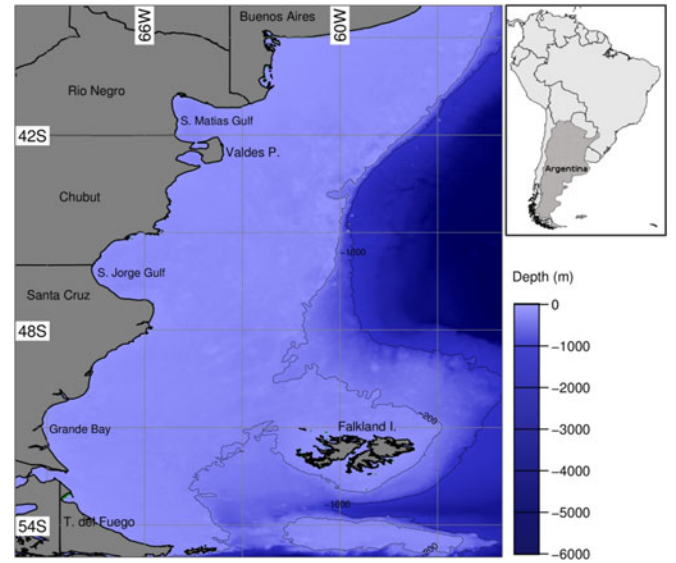


Fig. 1. Study region over PCS. Map depicts bathymetry and contours correspond to the 200 and 1000 m isobaths.

percentage of valid data. These procedures were carried out pixelwise to get maps of percentage of valid data and mapwise to obtain general statistics.

2) *Spatio-Temporal Variation and Anomalies:* To study the spatio-temporal variability of satellite chl-a concentration, we aggregated data with different temporal granularities (i.e., the whole study period, annually and monthly) using descriptive statistics, such as the average, median, standard deviation, minimum, and maximum values (we only show results on the average). As products are eight-day composites and they may start in one month and end in the following, we used the month of the start date in the eight-day composite to perform the monthly aggregations. We also built monthly climatologies, and estimated monthly and annual anomalies by subtracting from each temporal composite the corresponding climatology. Monthly climatologies were estimated aggregating all images (in different years) which start month was the same. Therefore, January climatology was built by aggregating (averaging in this case) all maps which start month was “01,” and so on. Annual anomalies in chl-a concentration for a given year, $Anomaly_y$, were estimated as

$$Anomaly_y = Average_y - Total_average \quad (1)$$

where $Average_y$ is the average chl-a concentration for year $y = 2003, \dots, 2013$ and $Total_average$ is the average chl-a concentration of the whole period. Monthly anomalies in chl-a concentration, on the other hand, were estimated as

$$Anomaly_{y,m} = Average_{y,m} - Climatology_m \quad (2)$$

where $Average_{y,m}$ is the average chl-a concentration for year $y = 2003, \dots, 2013$ and month $m = 1, 2, \dots, 12$ and $Climatology_m$ is the climatological average of chl-a concentration for the corresponding month m over all the years y .

3) *Gap-Filling*: For the reconstruction of missing data, we used Data INterpolation Empirical Orthogonal Functions decomposition (DINEOF) [15]. This is a self-consistent method for reconstructing missing values in oceanographic data sets. It is based on the fact that an optimal number of empirical orthogonal functions (EOFs) retains a large fraction of the total variance. The information contained in the dataset is used by the EOF series to infer the missing values. The DINEOF method fills the missing data by means of an iterative process. The method is robust and simple to use, the code is freely available and it does not need any *a priori* information about the statistical error of the data [15], [16]. It has proven to be successful in the reconstruction of gappy series of sea surface temperature (SST) and chl-a [16].

4) *Masking of Coastal Areas*: We masked coastal waters that surpassed the $Rrs667 = 0.0012 \text{ sr}^{-1}$ threshold ([13] and http://oceancolor.gsfc.nasa.gov/REPROCESSING/SeaWiFS/R4/masks_n_flags.html#SEC2). We counted the number of times each pixel in the series had a $Rrs667$ higher than 0.0012 sr^{-1} and decided to mask those that surpassed the threshold more than 75 times (i.e., at least 75 maps out of 506, $\approx 15\%$ of the whole period). This number was set arbitrarily as a tradeoff between masking coastal areas and not losing so much data. The total area masked consisted of 4200 pixels (4% of the area).

It is well known that empirical algorithms (of the blue-to-green ratio type) developed for Case 1 waters [17] fail in coastal zones due to the presence of mineral sediments brought by rivers or resuspended from the bottom, as well as by the presence of colored dissolved organic matter of terrestrial origin which result in a strong overestimation of satellite chl-a values [18]–[22]. As an example, results of a first validation of SeaWiFS-derived chlorophyll performed by Armstrong *et al.* [23] in the Río de la Plata (RDP) estuary and adjacent Argentine shelf waters located at $\approx 35 \text{ S}$ (a bit north of the present study area), showed that the satellite measures significantly overestimated near-surface chl-a in the RDP turbid waters (up to six times), but provided adequate estimates (within 10%) in the subtropical clear waters of the Brazil Current in the continental shelf. In turn, a match-up analysis in the Argentine shelf-break showed that SeaWiFS-derived spectral **normalized water-leaving radiances (nLw) are well related ($0.77 < r^2 < 0.98$) to *in situ* measurements, with higher correlation at lower wavelengths [19]. Therefore, by masking the coastal area, we avoid the influence of regularly high chlorophyll concentration values occurring in these areas and prevent a biased estimation of chl-a concentration when we spatially aggregated values for the whole study area.

5) *Phenological and Statistical Indexes*: Using the gap-filled time series, we estimated two phenological indexes: date of maximum concentration and bloom starting date (BSD), and also obtained statistical indexes such as minimum and maximum bloom areas, their occurrence date and bloom occurrence frequency. Herein, we describe them briefly.

a) *Date of Maximum Concentration*: This index corresponds to the date in which the maximum concentration of chl-a is observed. This index was obtained pixelwise for each year and for the whole study period.

TABLE I
MONTHLY CLIMATOLOGY IN THE PERCENTAGE OF VALID DATA

Month	Average (%)	Standard deviation	Minimum (%)	Maximum (%)
Jan	91.3	4.6	79.8	97.2
Feb	93.0	5.3	79.4	98.7
Mar	91.0	8.9	61.6	98.2
Apr	70.5	14.5	37.8	93.1
May	32.3	13.1	6.6	60.0
Jun	15.1	5.3	5.3	27.3
Jul	28.4	11.8	9.3	53.8
Aug	68.8	14.9	36.0	94.7
Sep	86.0	10.2	51.4	98.0
Oct	91.5	5.3	79.4	97.7
Nov	88.9	7.4	66.7	97.2
Dec	82.7	11.9	34.8	95.9

- b) *BSD*: BSD was obtained with two different methods: One based on the rate of change and the other one based on a threshold. The first method sets the BSD when the maximum rate of change (maximum slope between two successive maps) is observed (modified from [24]). For the second method, we followed [24] and we used a value of 5% above the median of the series (11 years) as threshold to determine bloom occurrence [25].
- c) *Bloom Frequency and Derivatives*: Using the threshold of 5% above the median as an estimate of bloom occurrence [25], we obtained statistical indexes such as the minimum and maximum bloom areas, their occurrence date and the frequency of bloom occurrence. To obtain bloom frequency per pixel, we classified all maps in the time series according to the threshold previously established. To get bloom frequency, we just counted per year and for the whole period, the times each pixel was classified as bloom. Then, we transformed that frequency into a percentage (to get a proxy for duration of blooms).

This study was carried out with free data and free and open source software (FOSS). The raster processing was done in GRASS GIS 7 [26], by means of new temporal modules [27]. We used R [28] combined with GRASS GIS through *rgrass7* package [29] for running DINEOF [15], [16] by means of package *sinkr* [30] and for estimating the BSD with the threshold method. This latter task was entirely programmed in R. Most of the workflow followed for this study is documented at: https://grasswiki.osgeo.org/wiki/Temporal_data_processing. DINEOF standalone software is freely available at: <http://modb.oce.ulg.ac.be/mediawiki/index.php/DINEOF>.

III. RESULTS

A. Availability of Valid Data

The percentage of valid data varied both within and between years. In general, we found that the percentage of valid data decreased southward. The lowest percentages of valid data on the shelf were observed in coastal areas of Santa Cruz, Tierra del Fuego and, the Falkland Islands. The monthly climatology in the percentage of valid data (see Table I) shows that the month

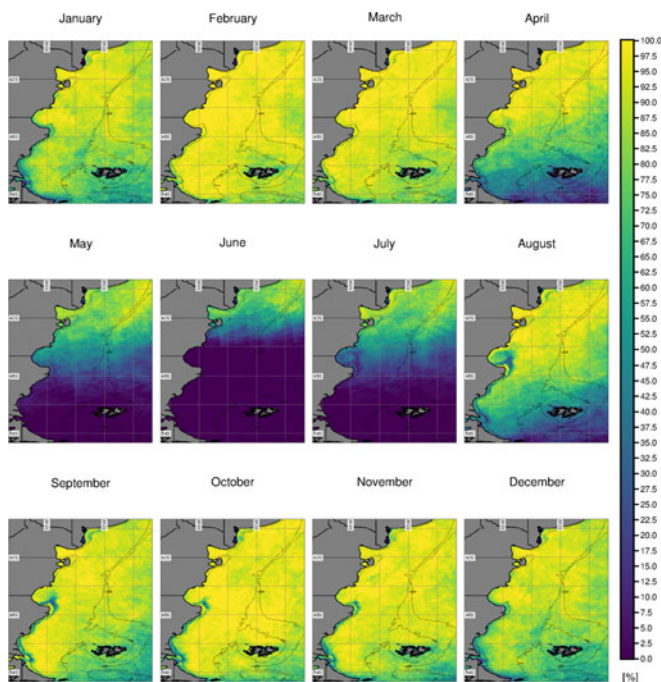


Fig. 2. Monthly climatology in the percentage of valid data in MODIS/Aqua L3 chlorophyll images over the period 2003–2013. The dotted line close to the coastline represents the limit of area masked by means of Rrs667. Contours correspond to the 200 and 1000 m isobaths.

with the lowest percentage of valid data is June with a 27%, followed by July (28.4%), and May (32.3%), coinciding with late austral autumn and early winter. The total lack of valid data at high latitudes in winter months is related to the solar angle and geometry of illumination.

Spatially, the lowest surface of valid data is observed between April and August, with June being the month showing the smallest area with valid data (see Fig. 2). On the other hand, the lack of valid data during austral summer months all along Santa Cruz coastline, starting at San Jorge Gulf and southwards seems to be an artifact of the processing itself, especially, the flagging of coccolithophorids (preliminary observations not presented here).

B. Spatial Variation and Climatologies

The results showed that mean chl-a concentration changed spatially during the cycle of a year and among years, both in values attained and in the distribution and extension of high concentration areas. However, a certain constancy was observed in the location and timing of phytoplankton maxima (bloom) occurrence. Monthly climatology (see Fig. 3) showed that mean chl-a concentration increases from September onwards in the northern part of the slope and midshelf until 44 S, and propagates toward the south, reaching maximum values and extent in October–November. Between August and October, the maximum chl-a progress from the outer edge of the platform to the coast. By December, the area with high values shrinks to the north, but enlarges southward, reaching 54 S. In January and February, high concentrations of chl-a ($\text{chl-a} \approx 3.0\text{--}5.0 \text{ mg/m}^3$)

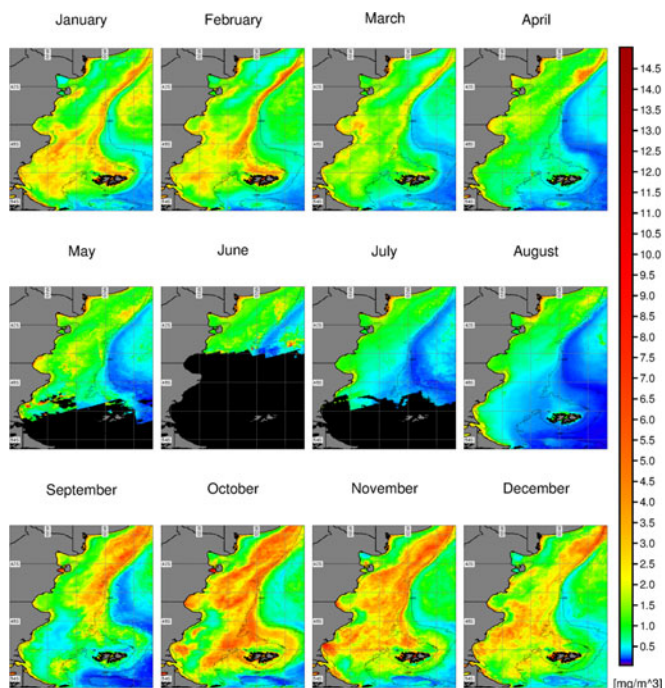


Fig. 3. Climatological monthly mean chl-a maps (mg/m^3) obtained from MODIS/Aqua L3 over the period 2003–2013. Black areas represent areas with no valid data and contours correspond to the 200 and 1000 m isobaths. The dotted line close to the coastline depicts the limit of the area masked by means of Rrs667.

are observed in quite distinct areas: a strip along the shelf-break, in Valdés front and coastal fronts north of the Falkland Islands and in midshelf south of 46 S. In March, high concentrations previously observed in the south, have almost disappeared and remain only over the shelf-break until 44 S and over the San Jorge Gulf front. In May, June, and July, a large proportion of the study area has total absence of valid data, which prevents to some extent the description of the average behavior of chl-a. However, mean values of $\approx 1.0 \text{ mg/m}^3$ are observed in the shelf (up to 46 S in July) and relatively lower values ($\text{chl-a} < 0.5 \text{ mg/m}^3$) southwards and off the shelf.

The time series constructed after spatially aggregating (i.e., average value of all the pixels in each map) chl-a across the study area (and having masked coastal areas) showed a marked annual cycle with higher values during austral spring (which persist during summer in varying degrees) and decreasing toward autumn–winter (see Fig. 4) as indicated by the monthly climatologies in the spatial dimension (see Fig. 3). It was also evident in these series, perhaps more clearly than in the spatial analysis, the presence of a second peak in the fall (March–April to June), usually (but not always) smaller than the spring peak (from September–October to December). This autumn peak was higher than the annual maximum in both 2010 and 2011, consistently with the monthly anomalies and the general pattern of positive anomalies recorded for those years (see Section III-C).

C. Anomalies

Both monthly and annual anomalies showed extensive variation in the average, minimum, and maximum chl-a

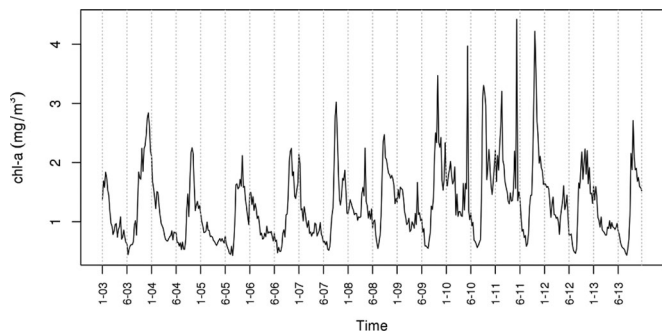


Fig. 4. Time series of mean chl-a concentration (mg/m^3) from MODIS/Aqua L3 images spatially aggregated every eight days over the period 2003–2013.

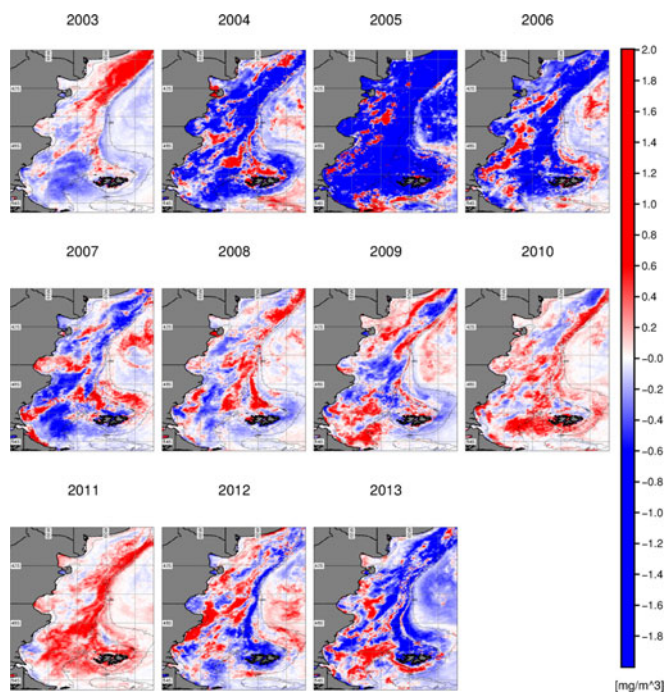


Fig. 5. Annual anomalies in mean chl-a concentration (mg/m^3) from MODIS/Aqua L3 images over the period 2003–2013. Contours correspond to the 200 and 1000 m isobaths. The dotted line close to the coastline represents the limit of the area masked by means of Rrs667.

concentrations attained, with years (and months) of large areas of positive anomalies and years (and months) of dominant negative anomalies. Fig. 5 shows mean annual anomalies.

Annual anomalies in the concentration of chl-a showed that there is no clear pattern in the occurrence of higher or lower than average concentrations, but a few years appear to be higher and others, lower. In addition, throughout the region and over the years the spatial distribution of positive and negative anomalies also changed. For example, in 2008, 2010, and 2011, positive anomalies are found all along the shelf-break, while in 2007, 2012, and 2013, the chl-a in that area is lower than the general average (negative anomaly). Particularly, year 2003 showed a large range of values higher than the overall average in the middle shelf and shelf-break north of 44 S. In 2004, we observed values lower than the average in most of the area, while from

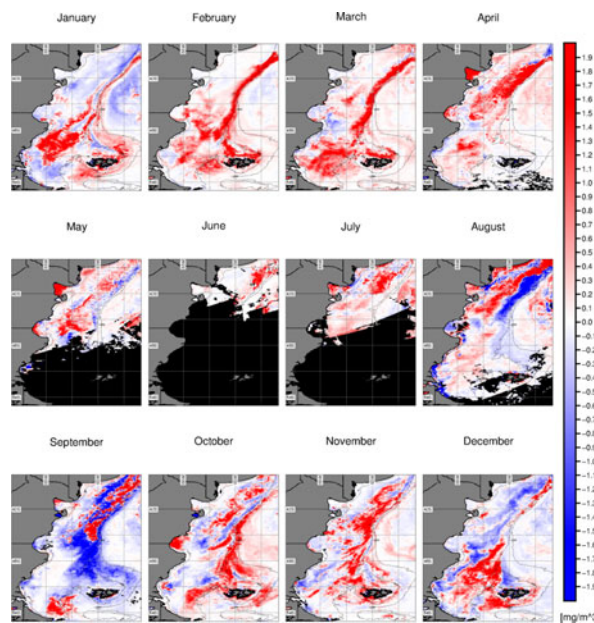


Fig. 6. Monthly anomalies in the mean chl-a concentration (mg/m^3) from MODIS/Aqua L3 images for the year 2011. Black areas represent areas with no valid data and contours correspond to the 200 and 1000 m isobaths. The dotted line close to the coastline represents the limit of the area masked by means of Rrs667.

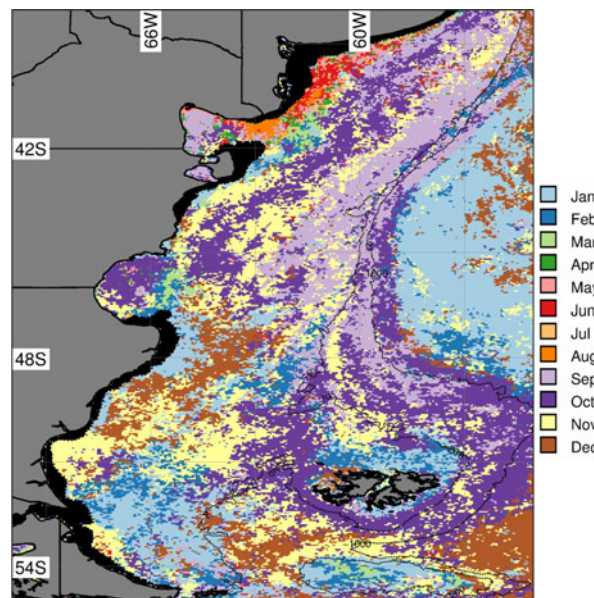


Fig. 7. Month of maximum chl-a concentration (mg/m^3) from MODIS/Aqua L3 images over the period 2003–2013. Black areas represent masked coastal waters and contours correspond to the 200 and 1000 m isobaths.

2007 the surface occupied by positive anomalies appeared to increase, reaching a maximum in 2011 (37% of the area). The pattern of values higher than the average over large areas of the continental shelf in 2003, 2010, and 2011, was also evident when estimating anomalies in the yearly maximum and minimum (not shown). On the other hand, between 2004 and 2006 included, chl-a showed lower annual mean values than the overall average, i.e., negative anomalies in most of the region.

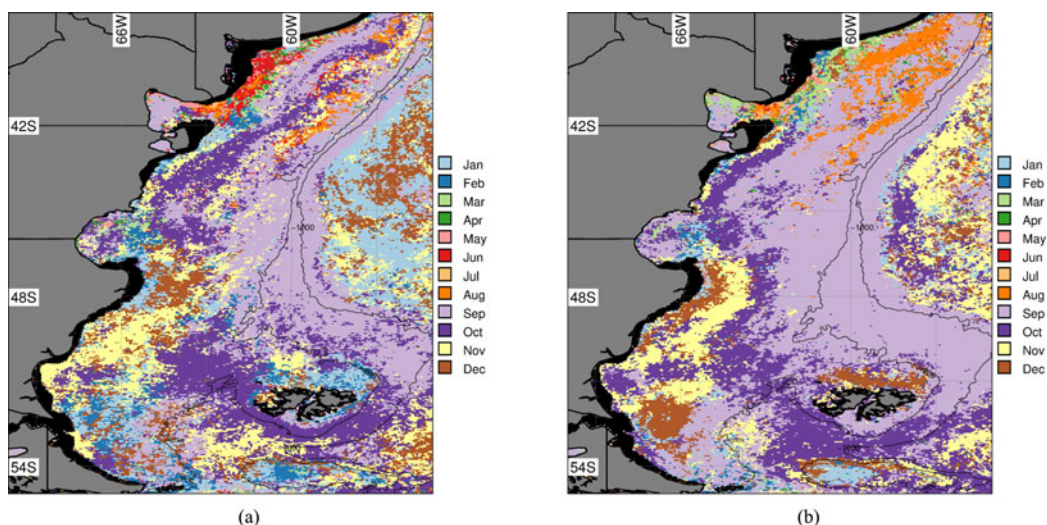


Fig. 8. Month of bloom start estimated as maximum rate of change (a) and based on a threshold of 5% above the median (b) chl-a concentration (mg/m^3). Black areas represent masked coastal waters and contours correspond to the 200 and 1000 m isobaths.

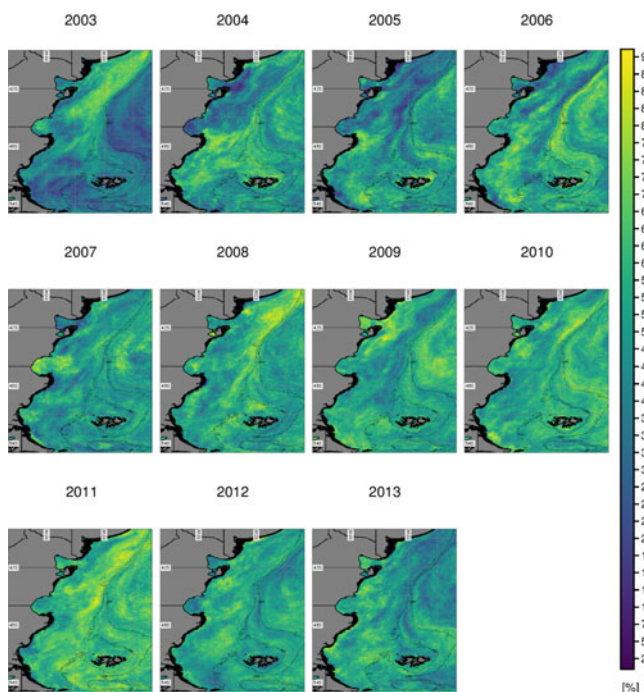


Fig. 9. Interannual variations in the percentage of bloom occurrence (2003–2013). Pixels with chl-a concentrations a 5% above the median of the series were classified as bloom. Black areas represent masked coastal waters and contours correspond to the 200 and 1000 m isobaths.

In 2005, in particular, these negative anomalies covered most of the study area, while in 2004 and 2006, they were located mostly on the patagonic continental shelf.

Positive monthly anomalies in mean, maximum, and minimum chl-a values were observed for those years that showed annual positive anomalies. For example, positive anomalies observed for 2011 (see Fig. 5) were associated with positive anomalies in almost every month of the year, especially notable

over the shelf-break and the southern platform, in February, March, and April (see Fig. 6).

D. Phenological and Statistical Indexes

The analysis of the occurrence of annual maximum (see Fig. 7) showed that approximately 66% of the area peaked between July and September (DOY 180 to 290), while only 11% did it in October (middle shelf, waters between 200 and 1000 m isobaths and Grande Bay, San Jorge Gulf, San Matías Gulf, and Nuevo Gulf tidal fronts).

With the method based on the maximum rate of change [see Fig. 8(a)], a 67% of the area showed a BSD ranging from August to mid October (DOY 212 and 287). Most of that area however (45%) began to bloom between September and early November (DOY 241–297). The central areas of midshelf, waters outside shelf south of 48 S and coastal tidal fronts near Santa Cruz province started blooming between late September and early November (DOY 260–310). In addition, interspersed with these areas, in midshelf, along the coastline and off the shelf-break, blooms began between July and August (DOY 180–240). Other areas around the coast showed earlier flowering dates in May and June. By means of the threshold method (see Fig. 8(b)), we observed that approximately 50% of the study area began to bloom between September and October (DOY 249 and 297). Particularly along the shelf-break and in most of the study area south of 44 S, blooms started during October (DOY 270–310). On the other hand, most of the area north of 44 S, started blooming by August (DOY 210–240).

Bloom area and bloom frequency varied among years, in coincidence with annual positive and negative anomalies, respectively, but in average most of the shelf showed bloom chl-a levels approximately half of the period considered. To some extent, this can provide information about the length of blooms. However, this methodology is not suited to distinguish whether there were one or two blooms (in the latter case the information provided would be the sum of the length of the two blooms).

These percentages (“duration”) changed both spatially and temporally (see Fig. 9). We observed that those years in which concentrations of chl-a were higher than long-term average, also showed a higher percentage of bloom occurrence, i.e., bloom level concentrations were maintained for a “longer” period. For example, the areas that showed the highest bloom length in 2003 were the same areas that denoted positive anomalies in the previous analysis and the same pattern was observed for 2011, when almost the entire study area had high levels of chl-a.

IV. DISCUSSION

The 11 years of MODIS/Aqua L3 data analyzed in this paper provide an overview of the evolution and the spatio-temporal variability of chl-a and phytoplankton blooms in the PCS. While other authors have presented similar analysis [3], [4], [31], this is the first time this MODIS product (standard empirical algorithm OC3Mv6, 8-day, ≈ 4 km) is used to analyze the spatial and temporal variations in the concentration of chl-a in a wide region over the Argentinian Sea, and for such a period of time. Previous studies covered shorter periods (1998–2003 or 1998–2004, respectively), and used data from sensors other than MODIS, especially SeaWiFS. On the other hand, [31] performed a similar analysis the southern coast of Buenos Aires province using MODIS/Aqua data but a nonstandard NASA chl-a algorithm, i.e., the Quasi-Analytical algorithm based on [32]. Besides, this is also the first time that bloom phenology indexes are estimated and their spatio-temporal variability is analyzed for this area.

In general, results demonstrated consistency with previous studies in terms of variations observed in former periods, both in satellite-derived chl-a and measured *in situ* [3], [4]. Therefore, regarding known issues in ocean color radiometry (atmospheric correction difficulties, overestimation in coastal areas, global versus regional models, lack of valid data in higher latitudes, etc.), MODIS satellite chl-a was capable of reproducing the spatio-temporal patterns of phytoplankton variability.

The spatial variability observed at each moment, or for the aggregation of a certain period, is likely to be dependent on the environmental differences among diverse areas and the particular dynamics associated to the geographic location. On the other hand, the intra-annual variability observed can be related to seasonal regular cycles in lightning conditions, nutrient flux, and vertical stratification, among others. The stratification of the water column is of particular relevance in the annual cycle of phytoplankton in the PCS. The thermocline varies seasonally: it develops in the spring (from September–October to December), intensifies in summer (December–January to March), declines in autumn (April to June) and disappears completely in winter (July to September) [33]. The seasonal evolution of the vertical stratification plays an important role in nutrient exchange with deeper layers and maintenance of phytoplankton on the surface. Rivas *et al.* [3] sustain that the chlorophyll maximum spreads from the outer edge of the platform to the coast, in accordance with the direction of development of the seasonal thermocline. This displacement direction was also evident in this study. Along the PCS, there are relatively small frontal areas associated with increased vertical circulation. This maintains high

concentrations of nutrients in the euphotic zone even after the spring bloom. As a result, the frontal areas are responsible for the high concentrations of chl-a found during the summer.

The interannual variability observed in chl-a concentration and percentage of bloom occurrence (proxy for bloom duration) might be related to external or extrinsic forces associated with climate change that may affect lightning conditions, stratification of the water column, flow of nutrients, etc. A high interannual variability in the concentration of chl-a was already described for the Argentine continental shelf and shelf-break [34], [35]. Wind anomalies that could cause upwelling and changes in the position of fronts, as well as anomalies in the discharge of large rivers as a consequence of higher precipitations are likely related to the anomalies observed in the concentrations of chl-a [4], [36]. For example, Signorini *et al.* [35] associated the great bloom of 2003 (which was also observed in the present study) with changes in the supply of nutrients, particularly iron, from different sources. Other authors have linked the interannual fluctuations of chl-a and the intensity of blooms to climatic phenomena such as North Atlantic Oscillation in the North Atlantic [37] or El Niño Southern Oscillation (ENSO) in the Southern hemisphere, both in river [38] and marine systems [34]. The mechanism by which these phenomena may produce such variations is still under study. Some authors suggest that the overall impact of ENSO on winds (in response to changes in sea temperature) can affect the distribution of phytoplankton [34], [39]. Others, however, argue that ENSO may cause a change in the composition of the phytoplankton community and/or the timing and intensity of phytoplankton blooms [38], [40]. In southeastern South America, the ENSO has strong effects on rainfall, especially in spring [41]. This would increase the discharge of large rivers such as the RDP during El Niño events, and reduce it during La Niña events [42]. An increase in the concentration of chl-a in areas surrounding the discharge of the RDP has been observed during El Niño events probably due to a larger extension of the river plume and an increased supply of nutrients to the shelf [36]. Machado *et al.* [34] analyzed monthly series of satellite chl-a from SeaWiFS sensor for the period 1997–2008. They observed positive anomalies in chl-a concentrations during El Niño events in areas north of 45 S and negative anomalies south of that latitude. The opposite pattern was recorded during La Niña events. In this study, however, the years of most significant positive anomalies (in terms of values attained, surface occupied, and duration of blooms) in most of the PCS (2010 and 2011) coincided with La Niña events (<http://www.ncdc.noaa.gov/teleconnections/enso/indicators/soi.php>). Only the first few months of 2010 showed negative values of the Southern Oscillation index. Further and deeper analysis would be required to explain these observations. The analyses of the relationships with variables such as SST, salinity, suspended matter, wind speed, and wind direction, as well as the search for possible relationships between phenological and statistical indexes with climate drivers, might provide a more complete view of the dynamics of the system.

In general, in most of the PCS, the annual maximum was observed between July and October. Maxima in winter are not

consistent with phytoplankton expected behavior for temperate shelves, but *in situ* studies have also shown that high concentrations might occur in July [11]. In this sense, there were some “caveats” likely associated with the methodology used (aggregation and search of maxima by calendar years, i.e., from January 1st to December 31st). Indeed, the maximum identified is the maximum of that period (the calendar year), but it is not known exactly whether these maxima correspond to bloom peaks in all cases (i.e., they might be noise, isolated maxima, etc.). It was observed when examining individual time series in random pixels that there were years that showed two primary blooms (because one of them occurred earlier or was delayed for some reason) but only the highest of them was identified as yearly maximum. One way to assess these results and probably achieve more unequivocal results would be to study the effect of systematically moving the beginning of the series to find the date in which the maximum value is more often observed [43]. That is, instead of aggregating from January 1st to December 31st, aggregate from February 1st to January 31st, then from March 1st to February 28th or 29th accordingly, etc., and extract the date of the maximum chl-a in each case.

The problems described above in the identification of date of maximum concentration affected then the determination of BSD by the threshold method, that departs from yearly maximum to find the beginning of a bloom [24]. In the case of two peaks in one calendar year, for example, the consequence was an overlook of the conditions that lead to that earlier or delayed (depending of the case) bloom. BSD as estimated from the threshold method had also other problems. For example, there were cases in which the BSD was the same date as the yearly maximum, since it was the first date after the threshold, or also cases in which no BSD was identified since the requirement of two time steps below the threshold was not met. The method to determine BSD by the maximum rate of change, on the other hand, was not influenced by the same kind of problems, but it is likely influenced by noise or intrinsic variability in the data. Besides, this method captures, by definition, the moment when the change is greater, i.e., when the bloom is already fully declared. It would be desirable, however, to identify the moment before that, in order to study the conditions or factors that lead to a bloom [24]. In general, both methods have flaws and difficulties to correctly address every particular case and they are not suited to identify the occurrence of secondary blooms. Further research is needed to find better methods or better tweaks to the methods used here, so they can be effective in a greater set of conditions.

Given the importance of phytoplankton in aquatic ecosystems, any change in the timing (beginning and duration) of blooms may have critical effects on the rest of the components system, as well as on global biogeochemical cycles and climate [1]. A recent study suggested that climate change may affect the timing of blooms [44], leading to a decrease in the synchronization between phytoplankton blooms and higher levels’ life cycles [45]. Changes in global climate can also affect the frequency of occurrence of events such as El Niño/La Niña, and thus influencing phytoplankton cycles. This possibility emphasizes the need to study the determinants of phytoplankton blooms and their vulnerability to climatic variability [46].

While satellite products have valuable advantages for this kind of studies, they also have some limitations. One of them is related to the uncertainty involved in the estimation of the biophysical parameter (chl-a in this case). In this sense, the performance of MODIS/Aqua NASA standard chl-a product in this region have been assessed in previous works. Mean absolute relative percentage errors for MODIS chl-a estimates found using OC3M algorithm were $\approx 40\%$ [12], [47] in the Argentinian Continental shelf and 60% in the shelf-break region [48]. We may therefore assume that satellites in general and MODIS/Aqua in particular, are capable of reproducing the spatio-temporal patterns of chl-a, even though, differences vary according to region considered [3]. Another source of uncertainty is related to the representativeness of climatological averages constructed from L3 data. A series of flags from L2 (incidence angle, clouds, coccolithophorids) limits the number of data upon which each eight-days product is built. In the particular case of PCS, percentage of missing data is highly significant in May, June, and July and this might influence higher order aggregations. We partially solved that by filling gaps using DINEOF algorithm. Last but not the least, there is another limitation associated with the accuracy of satellite estimations in coastal areas (also called optically complex waters or waters Case 2). In the Patagonian region, coastal waters receive great terrigenous contributions from several rivers that invalidate the empirical relationship between radiance and chl-a and lead to over-estimations of the chl-a algorithm. For this reason, we masked coastal areas before obtaining spatially aggregated averages.

V. CONCLUSION

With the analysis of these 11 years of this MODIS/Aqua L3 product, we obtained an overview of the evolution and the spatio-temporal variability of chl-a that in general and despite its limitations, was consistent with previous studies based on both satellite and *in situ* data. Therefore, this study complements, with up-to-date information, those previous baseline studies in the continental shelf and shelf-break of the Argentinean patagonic region and provide a first approach to the study of phenology of phytoplankton blooms in the area. The final goal is to use these kind of products to predict the occurrence of harmful algal blooms, the dynamics of marine system (under extractive pressure) and the effects of global changes over climatic and biogeochemical cycles.

Besides the results *per se*, the relevance of this study is also related to the use of a novel free and open source tool that provides the advantage of automating all (or most of) the processing, and which allows the application of the same methodology to analyze satellite time series of different variables, like SST.

ACKNOWLEDGMENT

This work was part of V. C. Andreo’s MS thesis and was funded by the Argentinian Spatial Agency (CONAE). The authors would like to thank NASA for making MODIS data freely available. We are also grateful to three anonymous reviewers

who provided valuable comments and suggestions on an earlier version of the manuscript.

REFERENCES

- [1] P. Falkowski, "Ocean science: The power of plankton," *Nature*, vol. 483, pp. S17–S20, 2012.
- [2] W. W. Gregg and C. S. Rousseaux, "Decadal trends in global pelagic ocean chlorophyll: A new assessment integrating multiple satellites, *in situ* data, and models," *J. Geophys. Res.: Oceans*, vol. 119, pp. 5921–5933, 2014.
- [3] A. Rivas, A. Dogliotti, and Gagliardini, "Seasonal variability in satellite-measured surface chlorophyll in the patagonian shelf," *Continental Shelf Res.*, vol. 26, pp. 703–720, 2006.
- [4] S. Romero, A. Piola, M. Charo, and C. Garcia, "Chlorophyll—A variability off patagonia based on SeaWiFS data," *J. Geophys. Res.*, vol. 111, 2006, Art. no. C05021.
- [5] A. A. Bianchi *et al.*, "Annual balance and seasonal variability of sea-air CO₂ fluxes in the Patagonia Sea: Their relationship with fronts and chlorophyll distribution," *J. Geophys. Res.*, vol. 114, pp. 2156–2202, 2009.
- [6] C. Campagna, F. Quintana, B. Le Boeuf, S. Blackwell, and D. Crocker, "Diving behaviour and foraging ecology of female southern elephant seals from patagonia," *Aquatic Mammals*, vol. 24, pp. 1–11, 1998.
- [7] W. W. Gregg, N. W. Casey, and C. R. McClain, "Recent trends in global ocean chlorophyll," *Geophys. Res. Lett.*, vol. 32, 2005, Art. no. L03606.
- [8] C. W. Brown and G. P. Podesta, "Remote sensing of coccolithophore blooms in the western South Atlantic Ocean" *Remote Sens. Environ.*, vol. 60, pp. 83–91, 1997.
- [9] C. A. E. Garcia *et al.*, "Environmental conditions and bio-optical signature of a coccolithophorid bloom in the patagonian shelf," *J. Geophys. Res.*, vol. 116, 2011, Art. no. C03025.
- [10] S. R. Signorini *et al.*, "Seasonal and inter-annual variability of calcite in the vicinity of the patagonian shelf break (38 S – 52 S)," *Geophys. Res. Lett.*, vol. 33, 2006, Art. no. L16610.
- [11] V. A. Lutz, A. Subramaniam, R. M. Negri, and J. I. Carreto, "Annual variations in bio-optical properties at the "Estación Permanente de Estudios Ambientales (EPEA)" coastal station, Argentina," *Continental Shelf Res.*, vol. 26, pp. 1093–1112, 2006.
- [12] A. I. Dogliotti, I. R. Schloss, G. O. Almandoz, and D. A. Gagliardini, "Evaluation of SeaWiFS and MODIS chlorophyll—A products in the argentinean patagonian continental shelf (38 S–55 S)," *Int. J. Remote Sens.*, vol. 30, pp. 251–253, 2009.
- [13] A. Morel, "Optical modeling of the upper ocean in relation to its biogenous matter content (Case I waters)," *J. Geophys. Res.: Oceans*, vol. 93, pp. 10749–10768, 1988.
- [14] N. Pahlevan, S. Sarkar, and B. A. Franz, "Uncertainties in coastal ocean color products: Impacts of spatial sampling," *Remote Sens. Environ.*, vol. 181, pp. 14–26, 2016.
- [15] J.-M. Beckers and M. Rixen, "EOF calculations and data filling from incomplete oceanographic datasets," *J. Atmospheric Oceanic Technol.*, vol. 20, pp. 1839–1856, 2003.
- [16] A. Alvera-Azcrate, A. Barth, M. Rixen, and J. Beckers, "Reconstruction of incomplete oceanographic data sets using empirical orthogonal functions: application to the Adriatic sea surface temperature," *Ocean Modell.*, vol. 9, no. 4, pp. 325–346.
- [17] A. Morel and L. Prieur, "Analysis of variations in ocean color," *Limnology Oceanography*, vol. 22, pp. 709–722, 1977.
- [18] IOCCG, "Remote sensing of ocean color in coastal, and other optically complex waters." in *Reports of the International Ocean-Color Coordinating Group*, V. Stuart, Ed. Int. Ocean-Colour Coordinating Group: Dartmouth, NS, Canada, 2000.
- [19] C. A. Garcia, V. M. Garcia, and C. R. McClain, "Evaluation of SeaWiFS chlorophyll algorithms in the Southwestern Atlantic and Southern Oceans," *Remote Sens. Environ.*, vol. 95, pp. 125–137, 2005.
- [20] M. Darecki, S. Kaczmarek, and J. Olszewski, "SeaWiFS ocean colour chlorophyll algorithms for the southern Baltic Sea," *Int. J. Remote Sens.*, vol. 26, pp. 247–260, 2005.
- [21] G. Volpe *et al.*, "The colour of the Mediterranean Sea: Global versus regional bio-optical algorithms evaluation and implication for satellite chlorophyll estimates," *Remote Sens. Environ.*, vol. 107, pp. 625–638, 2007.
- [22] D. D'Alimonte, G. Zibordi, T. Kajiyama, and J.-F. Berthon, "Comparison between MERIS and regional high-level products in European seas," *Remote Sens. Environ.*, vol. 140, pp. 378–395, 2014.
- [23] R. A. Armstrong *et al.*, "Validation of SeaWiFS-derived chlorophyll for the Río de la Plata Estuary and adjacent waters," *Int. J. Remote Sens.*, vol. 25, pp. 1501–1505, 2004.
- [24] S. R. Brody, M. S. Lozier, and J. P. Dunne, "A comparison of methods to determine phytoplankton bloom initiation," *J. Geophys. Res.: Oceans*, vol. 118, pp. 2345–2357, 2013.
- [25] D. A. Siegel, S. C. Doney, and J. A. Yoder, "The North Atlantic spring phytoplankton bloom and Sverdrups critical depth hypothesis," *Science*, vol. 296, pp. 730–733, 2002.
- [26] GRASS Development Team, Geographic Resources Analysis Support System (GRASS). Software, version 7.1, 2016.
- [27] S. Gebbert and E. Pebesma, "A temporal GIS for field based environmental modeling," *Environ. Modell. Softw.*, vol. 53, pp. 1–12, 2014.
- [28] R Core Team, *R: A Language and Environment for Statistical Computing*, R Foundation for Statistical Computing, 2015.
- [29] R. Bivand, "rgrass7: Interface Between GRASS 7 Geographical Information System and R," *R package version 0.1-4*, 2016.
- [30] M. Taylor, "sinkr: Collection of functions with emphasis in multivariate data analysis," R package version 1.2.1, 2016.
- [31] A. L. Delgado *et al.*, "Seasonal and Inter-annual analysis of chlorophyll-a and inherent optical properties from satellite observations in the inner and mid-shelves of the South of Buenos Aires Province (Argentina)," *Remote Sens.*, vol. 7, pp. 11821–11847, 2015.
- [32] Z. Lee, K. L. Carder, and R. A. Arnone, "Deriving inherent optical properties from water color: A multiband quasi-analytical algorithm for optically deep waters," *Appl. Opt.*, vol. 41, pp. 5755–5772, 2002.
- [33] A. L. Rivas and A. R. Piola, "Vertical stratification at the shelf off northern patagonia," *Continental Shelf Res.*, vol. 22, pp. 1549–1558, 2002.
- [34] I. Machado, M. Barreiro, and D. Calliari, "Variability of chlorophyll-a in the Southwestern Atlantic from satellite images: Seasonal cycle and ENSO influences," *Continental Shelf Res.*, vol. 53, pp. 102–109, 2013.
- [35] S. R. Signorini *et al.*, "Further studies on the physical and biogeochemical causes for large inter-annual changes in the patagonian shelf spring-summer phytoplankton bloom biomass," Goddard Space Flight Center, Greenbelt, MD, USA, Tech Rep. NASA-TM 214176, 2009, p. 43.
- [36] C. Garcia and V. T. M. Garcia, "Variability of chlorophyll-a from ocean color images in the La Plata continental shelf region," *Continental Shelf Res.*, vol. 28, pp. 1568–1578, 2008.
- [37] S. Henson, R. Lampitt, and D. Johns, "Variability in phytoplankton community structure in response to the North Atlantic Oscillation and implications for organic carbon flux," *Limnology Oceanography*, vol. 57, pp. 1591–1601, 2012.
- [38] L. C. Solari *et al.*, "Phytoplankton chlorophyte structure as related to ENSO events in a saline lowland river (Salado river, Buenos Aires, Argentina)," *Ecol. Evol.*, vol. 4, pp. 918–932, 2014.
- [39] J. Li and A. Clarke, "Coastline direction, inter-annual flow, and the strong El Niño currents along Australia's nearly zonal southern coast," *J. Phys. Oceanography*, vol. 34, pp. 2373–2381, 2004.
- [40] F. D'Ortenzio, D. Antoine, E. Martinez, and M. Ribera d'Alcal, "Phenological changes of oceanic phytoplankton in the 1980s and 2000s as revealed by remotely sensed ocean-color observations," *Global Biogeochemical Cycles*, vol. 26, 2012, Art. no. GB4003.
- [41] A. Grimm, V. Barros, and M. Doyle, "Climate variability in Southern South America associated with El Niño and La Niña events," *J. Climate*, vol. 13, pp. 31–58, 2000.
- [42] A. Piola, S. Romero, and U. Zajaczkowski, "Space-time variability of the Plata plume inferred from ocean color," *Continental Shelf Res.*, vol. 28, pp. 1556–1567, 2008.
- [43] M.-F. Racault, C. Le Qur, E. Buitenhuis, S. Sathyendranath, and T. Platt, "Phytoplankton phenology in the global ocean," *Ecol. Indicators*, vol. 14, pp. 152–153, 2012.
- [44] M. Kahru, V. Brotas, M. Manzano-Sarabiaz, and B. Mitchell, "Are phytoplankton blooms occurring earlier in the Arctic?" *Global Change Biology*, vol. 17, pp. 1733–1739, 2011.
- [45] M. Edwards and A. J. Richardson, "Impact of climate change on marine pelagic phenology and trophic mismatch," *Nature*, vol. 430, pp. 430–481, 2004.
- [46] M. Vargas, C. W. Brown, and M. R. P. Sapiano, "Phenology of marine phytoplankton from satellite ocean color measurements," *Geophys. Res. Lett.*, vol. 36, no. 1, 2009, Art. no. L01608.
- [47] A. I. Dogliotti, V. A. Lutz, and V. Segura, "Estimation of primary production in the southern Argentine continental shelf and shelf-break regions using field and remote sensing data," *Remote Sens. Environ.*, vol. 140, pp. 497–508, 2014.

- [48] C. A. E. Garcia *et al.*, "Bio-optical studies along the Patagonian shelf-break zone," presented at the Ocean Optics XIX Conf., Barga, Italy, 2008, Paper 603.



Verónica Carolina Andreo (M'14) received the Ph.D. degree in biological sciences from the National University of Río Cuarto in 2012, and the M.Sc. degree in spatial applications for early warning and response to emergencies from the National University of Córdoba, Córdoba, Argentina, in 2015.

She is currently a Postdoctoral Researcher at the Faculty of Geo-Information Science and Earth Observation, University of Twente, Amsterdam, The Netherlands. Her main interests include remote sensing and GIS-based methods applied to disease

ecology, as well as, free and open source software for geospatial applications.



Ana I. Dogliotti received the Ph.D. degree in biology from the University of Buenos Aires, Buenos Aires, Argentina, in 2007.

She is an Adjunct Research Member of Consejo Nacional de Investigaciones Científicas y Técnicas, working at the Instituto de Astronomía y Física del Espacio, Buenos Aires, Argentina, where she is the Team Leader of the Marine Division of the Quantitative Remote Sensing Group. Her research interests include ocean color remote sensing research and applications.



Carolina Beatriz Tauro received the Licenciata degree in physics from the University of Córdoba, Córdoba, Argentina, in 2004, and the Ph.D. degree in physics in 2012.

Since 2009, she has been employed with Comisión Nacional de Actividades Espaciales (CONAE), Caba, Argentina, where she contributed in the Flight Engineering Group and the Science Team of the SAC-D/Aquarius Satellite, specially in the development of the L2 Microwave Radiometer applications. She is currently working on the development of future CONAEs satellite missions focused on ocean color. She has been a Professor at the University of Cordoba since 2004 and at present, she is a Professor in the Master of Spatial Information** Applications, Gulich Institute (CONAE and University of Córdoba). Her research interests include satellite microwave and optical remote sensing, related to geophysical retrieval algorithms.